Creep of Geotextiles Using Time–Temperature Superposition Methods

Jorge G. Zornberg, M.ASCE[1]; Brett R. Byler[2]; and Justin W. Knudsen[3]

Abstract: A temperature-accelerated tensile testing program was conducted in this study to characterize a woven polypropylene geotextile regarding its long-term stress–strain response, creep failure, and tensile strength remaining after sustained creep loading. Specimens were tested in a load frame that allowed control of multistage load paths. Consistent with current standards for rapid loading of geotextiles, roller-type grips capable of accommodating wide-width (200-mm) specimens were used in this study. The test program included: (i) Rapid loading tensile tests at room and elevated temperatures; (ii) conventional and temperature-accelerated creep tests; and (iii) rapid loading tensile tests conducted after sustained creep loading. Creep strain data for periods beyond 100 years were collected at various load levels using 8-h long tests involving the stepped isothermal method. The creep–failure curve, traditionally defined as time to rupture for sustained creep loading at various load levels, was defined in this study as the deviation of the creep curve from linear behavior in a semilogarithmic scale. A new approach was implemented to quantify and reference the residual tensile strength obtained from rapid loading at elevated temperatures of specimens that had been subjected to sustained creep. In spite of the significant slope in the creep-failure curve of the geosynthetic tested in this study, the residual tensile strength exceeds 90% of the ultimate tensile strength. An alternative to the current design approach, which involves use of creep-failure curves to define creep reduction factors is proposed. This involves use of creep-induced tensile strength loss, creep failure, and creep strains in the design of reinforced soil structures.

DOI: 10.1061/(ASCE)1090-0241(2004)130:11(1158)

CE Database subject headings: Earth reinforcement; Creep; Residual strength; Geosynthetics; Stress strain relations; Tensile strength.

Introduction

The tensile strength that should be used in the design of geosynthetic reinforced soil (GRS) structures is a significant, though controversial, aspect in current geotechnical practice. Current limit equilibrium design procedures for GRS structures use allowable tensile strength values that are significantly below the ultimate tensile strength, T_{ult,T_0}, determined from wide-width tensile tests conducted at room temperature, T_0. Reduction factors accounting for creep, installation damage, and degradation are used to penalize the ultimate tensile strength in order to define the allowable reinforcement tensile strength. Among the several reduction factors, the factor for creep is the largest since creep reduction factors as high as 5.0 are applied to T_{ult,T_0} depending on the polymer type. Accordingly, the design tensile strength may be as low as 20% of T_{ult,T_0} to account for creep alone.

The creep–rupture curve defines the time to rupture of geosynthetic reinforcements subjected to a constant sustained load. Current design guidelines in the U.S. (e.g., Elias et al. 2001) recommend that the creep–rupture curve be used to define the creep reduction factor RF_{CR}. Specifically, RF_{CR} is defined as the ratio between the creep–rupture load ($T_{CR,R}$) leading to rupture for a given design life (t_{dl}) and T_{ult,T_0} of the reinforcement. As the design life of reinforced structures may exceed 100 years, conventional creep tests are impractical for determining the creep–rupture curve, especially under low load levels. However, long-term data can be obtained from short-term tests using time–temperature superposition techniques. Among them, the stepped isothermal method (SIM) is particularly suitable as it avoids the use of multiple specimens for creep characterization (Thornton et al. 1998a, b).

While $T_{CR,R}$ may be significantly less than T_{ult,T_0}, the tensile strength of polymeric reinforcements loaded to rupture after sustained periods of creep has been reported to be only slightly below T_{ult,T_0}. This was the case in a study conducted in 1995, which evaluated the stability of a GRS structure built to stabilize steep landfill slopes in a hazardous waste site (GeoSyntec 1996; Zornberg and Kavazanjian 2001). The testing program in that study included wide-width tensile tests and creep tests followed by rapid loading to rupture. The main objective was to address concerns that sudden loading after sustained creep may have reduced the allowable strain and the ultimate tensile strength of the geogrid to values below those obtained from wide-width testing. Fig. 1 presents some results from that study, which included conventional wide-width tests (ASTM D4595, ASTM 1986) and multistage tests involving initial rapid loading, constant loading (creep), and rapid postcreep reloading. As observed in Fig. 1, during the rapid reloading that followed the creep period, the geogrid initially shows a higher stiffness than the one observed in

[1]Clyde E. Lee Assistant Professor, University of Texas at Austin, Austin, TX 78731.

[2]Project Engineer, Golder Associates, Lakewood, CO 80228.

[3]Former Graduate Student, Univ. of Colorado at Boulder, Boulder, CO 80309.

Note. Discussion open until April 1, 2005. Separate discussions must be submitted for individual papers. To extend the closing date by one month, a written request must be filed with the ASCE Managing Editor. The manuscript for this paper was submitted for review and possible publication on April 29, 2003; approved on August 14, 2003. This paper is part of the ***Journal of Geotechnical and Geoenvironmental Engineering***, Vol. 130, No. 11, November 1, 2004. ©ASCE, ISSN 1090-0241/2004/11-1158–1168/$18.00.

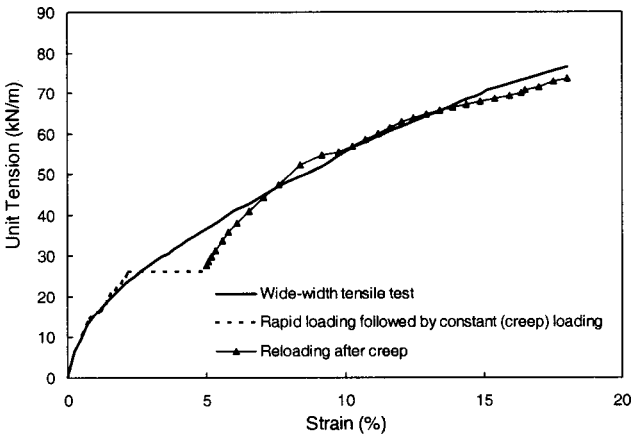

Fig. 1. Response of a polypropylene geogrid loaded rapidly to failure after a period of sustained creep

the wide-width (control) test at an equivalent tensile load. However, the postcreep reloading portion of the test eventually matches the wide-width (control) curve. Both the wide-width (control) curve and the creep/reloading curve fail at approximately the same ultimate tensile strength and show a similar strain level at rupture. These results provided the experimental information needed to calculate the maximum geogrid strains expected within the structure after construction, long-term differential settlement, and earthquake loading.

Orsat et al. (1998) and Greenwood et al. (2001) provided experimental data indicating that the tensile strength of polyester geogrids and individual polyester yarns retain most of the ultimate tensile strength following long periods of creep loading, even for strain levels approaching creep rupture. The term residual strength was used to describe the tensile strength available after a period of sustained creep loading. While there is general consensus that the residual strength of geosynthetics can be used in the analysis of structures subjected to rapid load events (e.g., earthquakes), no agreement has been reached as to how to incorporate residual strength concepts in static design (e.g., to define a creep reduction factor).

The scope of the testing program conducted in this study includes three test phases: (i) Rapid wide-width tensile testing conducted at both room and elevated temperatures; (ii) conventional and accelerated creep testing conducted using time–temperature superposition techniques (SIM); and (iii) multistage tests involving initial rapid loading, subsequent creep loading, and final rapid loading to rupture. The different phases of this experimental program used wide (200-mm) specimens and roller-type grips to achieve results consistent with wide-width tensile tests. Wide-width tests (ASTM 1986) simulate field conditions by minimizing contraction exhibited in the testing of narrow geotextile specimens ("necking"). Boundary effects have been reported to be minimized where using specimens approaching 200-mm width (Leshchinsky and Fowler 1990).

The overall objective of this study is to evaluate the creep deformations, creep failure, and residual tensile strength of geosynthetics using accelerated time–temperature procedures and procedures consistent with rapid tensile testing (e.g., wide specimens and roller grips). Previous test programs using the SIM were performed on individual yarns, tendons, geogrid ribs, or 50-mm wide geotextile specimens. While the need for using wide geotextile specimens with the SIM has been recognized, the use of comparitively wide specimens with the SIM has not yet been evaluated. Polypropylene (PP) geosynthetics were selected in this study because of the significant creep deformations exhibited by this polymer type and the lack of reported experimental data on accelerated creep for woven PP geotextiles. This study proposes new definitions for the quantification of creep (creep index), of creep failure (deviation of the creep curve from linear behavior in a semilogarithmic scale), and of the reference strength for quantification of residual strength. Design implications are finally proposed regarding the use of a creep reduction factor to account for the actual (comparatively small) loss in tensile strength after sustained creep while still accounting for creep failure.

Stepped Isothermal Method

The stepped isothermal method (SIM) relies on time–temperature superposition concepts for the characterization of viscoelastic properties of polymeric materials. While only creep behavior is characterized in this investigation, the SIM is also applicable to other viscoelastic mechanisms (e.g., stress relaxation). The SIM involves loading of a single specimen, which is subjected to a series of timed isothermal exposures at elevated temperatures in a stepped fashion (Thornton et al. 1998a). The use of a single specimen eliminates concerns related to specimen variability, which have been observed when using conventional time-temperature superposition techniques involving different specimens tested at different temperature exposures. Four 2-h isothermal exposures were used in this study (24, 38, 49, and 60°C) for each test. These 8-h long tests led to creep data corresponding to periods ranging from dozens to hundreds of years.

The fundamental premise of SIM testing is that viscoelastic processes are accelerated at elevated temperatures in a predictable manner. The Arrhenius equation provides the basis for the relation between the rate of reaction and temperature. On the other hand, the Williams–Landel–Ferry (WLF) equation and Boltzmann superposition principle provide justification for scaling and shifting strain data obtained at each isothermal exposure in order to define a master creep curve corresponding to the reference (room) temperature.

Arrhenius Equation

The Arrhenius equation, based on "rate-process theory", describes the relation between the rate of reaction and temperature for many physical and chemical reactions. A common form of the equation is (Koerner et al. l992):

$$k = k_0 e^{-(E/RT)} \tag{1}$$

where k=kinetic reaction rate; k_0=rate constant; E=activation energy; R=universal gas constant; and T=absolute temperature.

In this case, the rate of reaction corresponds to the creep strain rate, $\dot{\varepsilon}$. Although the Arrhenius equation describes the rate of reaction, time is not explicitly included as a variable. Eq. (1) can be rearranged by comparing the ratio of strain rate, $\dot{\varepsilon}_1$, at temperature T_1, to strain rate, $\dot{\varepsilon}_2$, at temperature T_2 as follows:

$$\ln\left(\frac{\dot{\varepsilon}_1}{\dot{\varepsilon}_2}\right) = \frac{E}{R}\left(\frac{1}{T_2} - \frac{1}{T_1}\right) \tag{2}$$

Eq. (2) can be used to predict the creep strain rate at a reference (room) temperature from the creep strain rate measured at an elevated temperature. The Arrhenius equation assumes that the viscoelastic mechanism (e.g., creep) remains unchanged at el-

evated temperatures. Consequently, material phase transitions such as the glass transition temperature should not be traversed, in principle, when testing geosynthetics. The activation energy is assumed to remain constant. As the activation energy is a function of temperature, temperature jumps during SIM testing should be made in a short period of time.

Williams–Landel–Ferry Equation

A procedure for shifting data obtained at elevated temperatures to a reference temperature was developed by Williams, Landel, and Ferry (Ferry 1980). Specifically, the WLF equation introduces a time shift factor, a_T, to relate strains at different temperatures. The shift factor, a_T, is the ratio between the time for a viscoelastic process to proceed at an arbitrary temperature and the time for the same process to proceed at a reference temperature:

$$\varepsilon_0(T_0,t) = \varepsilon\left(T, \frac{t}{a_T}\right) \tag{3}$$

where ε_0=strain at reference temperature; T_0=reference temperature; t=time; ε=strain at elevated temperature; T=elevated temperature; and a_T=shift factor.

The shift factor, a_T, is described by the empirical WLF equation as (Ferry 1980):

$$\log(a_T) = \frac{-C_1(T-T_0)}{(C_2+T-T_0)} \tag{4}$$

where C_1 and C_2=empirical constants.

Thus, creep strain measured at various isothermal steps during a SIM test can be shifted to form a master creep curve. The empirical constants C_1 and C_2 are a function of the polymer type and the reference temperature, T_0. Use of the WLF equation to quantify strain shifts is discussed in detail by Farrag (1998).

Boltzmann Superposition Principle

The Boltzmann superposition principle indicates that the strain response from distinct loading events can be superimposed to determine the total strain response corresponding to a single loading event. Although the load remains unchanged during SIM creep testing, each temperature step can be considered a discrete loading event since the creep mechanism is accelerated at elevated temperatures. The Boltzmann superposition principle assumes that:

1. The strain behavior of the material depends on its complete loading history.
2. Each load (or temperature exposure) is an independent event.
3. The total strain is the sum of the strains from each independent event.

Generation of Master Creep Curves Using the Stepped Isothermal Method

A master creep curve describes the long-term creep behavior at a reference temperature. The master creep curve can be defined by composing into a single curve the creep responses measured at different isothermal exposures during SIM testing. The procedure for generating a master creep curve using SIM data involves scaling and shifting creep data from each isothermal exposure. Fig. 2(a) presents the raw data for a specimen tested under a constant load equal to 30% of T_{ult,T_0}. The creep strains are shown in the figure as a function of time at each temperature step.

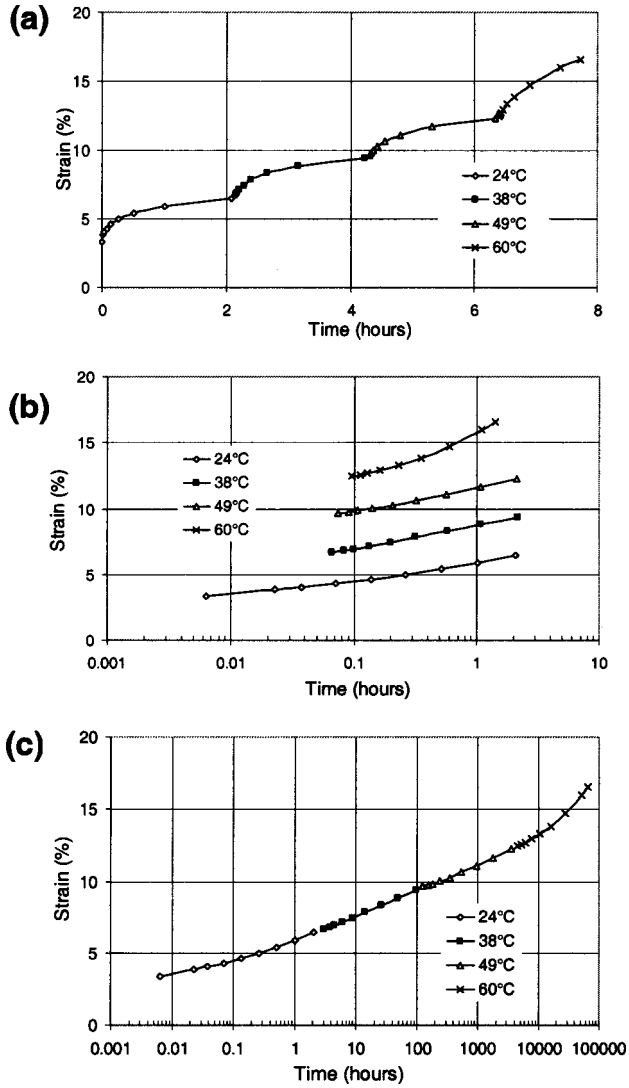

Fig. 2. Generation of master creep curve using the stepped isotherm method for a load of 30% of $T_{\text{ult},T0}$: (a) raw creep data, (b) scaled creep data, and (c) master creep curve

The raw data at each temperature exposure is first scaled to the reference temperature by subtracting a reference time from the real time for each elevated temperature data point. A shift time is selected so that the final slope of a strain–time curve at a specific temperature step matches the initial slope of the strain–time curve at the subsequent temperature step. This empirical scaling technique is consistent with the Arrhenius equation and the WLF equation. The shift factor described by the WLF equation [Eq. (4)] justifies the use of a shift time to relate the creep responses of a geosynthetic at different temperatures. The shifts, however, are defined empirically. The slope of the creep–time curve corresponds to the creep strain rate, thus creep data at each temperature exposure is scaled so that the strain rate corresponds to that of the reference temperature [Eq. (2)]. The scaled data plotted on a semilogarithmic scale are presented in Fig. 2(b). While previous studies have typically used temperature jumps of 7°C, the use of larger temperature jumps (11°C) in this study resulted in good matching of the slope of strain–log time curve segments.

The scaled creep–time curve segments corresponding to the reference temperature in Fig. 2(b) can be shifted horizontally to obtain a master creep curve. The Boltzmann superposition prin-

ciple justifies forming the master creep curve [Fig. 2(c)] by superimposing the creep strain responses measured at different temperatures. Thornton et al. (1998a) provides an in-depth discussion of scaling and shifting SIM data.

Materials, Equipment, and Methods

A woven PP geotextile with a mass per unit area of 492 g/m^2 was selected for this investigation. PP was chosen because of its significant creep susceptibility when compared to that of other polymers, such as polyester (PET). The low glass transition temperature of PP, which is below typical service temperatures, explains its comparatively high creep susceptibility. On the other hand, the glass transition temperature of PET is above typical service temperatures, which justifies its comparatively low creep susceptibility.

The testing program was performed using a Satec 60CG load frame with a 270 kN load capacity. This equipment provided the versatility needed to perform rapid loading wide-width tensile tests as well as multistage tests involving sequences of rapid loading and creep loading under controlled temperature conditions.

Roller grips were used for gripping the specimen, a temperature controlled environmental chamber was used for the accelerated (SIM) creep testing, and a linear variable differential transformer (LVDT) was used for measurement of specimen displacement. The 100-mm diameter roller grips selected for this study were designed to accommodate 200-mm wide specimens. The primary concern when selecting grips types is the tensile strength of the test material (GRI 1997). Roller grips have proven to perform well for testing high tensile strength woven geotextiles (Myles and Carswell 1986; GRI 1997). In addition, roller grips minimize stress concentrations at the grip and promote uniform tension throughout the specimen.

An environmental chamber with temperature insulating walls was constructed to enclose the roller grips and test specimens. The environmental chamber houses 1900 and 500 W electrical resistance strip heaters used to achieve temperature jumps of 11°C in a few minutes as well as to maintain a constant temperature during creep loading. The environmental chamber is relatively large, as it needs to accommodate the 200-mm wide specimens and grips. Care was taken to prevent direct exposure of specimens to the heating elements. Temperature was controlled using a Fuji Electric PXV3 proportional integral differential temperature controller with fuzzy logic capabilities equipped with a *T*-type thermocouple. Thermocouples for temperature control and for data acquisition were positioned close to the specimen, yet away from the heating elements. Three fans were used within the environmental chamber to enhance air circulation and promote uniform temperature. The environmental chamber and temperature control system was able to maintain constant temperature (±1°C). Because of the comparatively large thermal mass of this system, temperature jumps were achieved in approximately 4 min.

Displacements between reference points in the specimen were measured using an external LVDT (Schaevitz Model 1000 HR-DC). The LVDT, which was directly mounted to the specimen, has a linear range of ±25 mm. Geotextile strains up to 50% could be measured with a LVDT gauge length of 100 mm. Since the LVDT measurements are temperature sensitive, temperature corrections were applied to the displacement data. Temperature, displacements, and tensile load data were recorded at user-defined times using an automatic data acquisition system. Data were collected as follows:

1. During rapid initial loading, readings were taken every second to preserve the ramp-up loading (rather than taking initial strain readings at the onset of creep).
2. During sustained creep, reading frequency depended on the creep strain rate. During periods of high strain rates (e.g., during temperature jumps and initial stages of each isothermal temperature exposure), readings were taken every second. As the creep strain rate decreased, readings were taken at a maximum time interval of 1 min.
3. During rapid loading following sustained creep, readings were taken every second to adequately capture the stress–strain response until rupture.

The programming language *LABVIEW* was used as an interface to provide real–time stress–strain and temperature data. All tests were conducted using specimens from the same roll, and were performed using the same load frame, instrumentation, specimen preparation procedures, and initial loading procedures. Testing was conducted in the machine direction of the geotextile specimens. Since wide specimens (200-mm) were used throughout the testing program, sampling and conditioning procedures of the different tests were always conducted in general agreement with wide-width tensile testing standards ASTM D4595 (ASTM 1986). A PET geotextile was placed between the specimen and the roller grips to minimize friction and facilitate slippage of the PP specimen around the roller drum during loading. This approach facilitated obtaining a uniform strain rate and a smooth stress–strain curve. A preload of 222 N (approximately 1% of T_{ult,T_0}) was applied prior to each test to condition the specimen and minimize "settling in" of the stress–strain curve. The LVDT was mounted directly to the specimen upon completion of preloading.

Results and Analysis

The testing program conducted in this study involved: (i) Rapid loading wide-width tensile testing at ambient room temperature, (ii) rapid loading wide-width tensile testing at elevated temperatures, (iii) conventional creep tests at ambient room temperature, (iv) accelerated (SIM) creep tests conducted to characterize creep strain and to define creep failure, and (v) multistage (rapid loading and accelerated) creep tests conducted to rupture to define the geotextile residual tensile strength.

Characterization of Rapid Loading at Room Temperature

Wide-width tensile tests were performed at room temperature, T_0 (24°C±1°C), to obtain the ultimate tensile strength, T_{ult,T_0}. These tests allowed characterization of the material tensile strength and quantification of the material variability. Wide-width tensile tests were performed according to ASTM D4595 (ASTM 1986).

An average T_{ult,T_0} of 80.5 kN/m was obtained from eight wide-width tensile tests performed at room temperature. The standard deviation of T_{ult,T_0} for the eight tests was 1.9 kN/m and the coefficient of variability was 2.4%, indicating very good test repeatability. ASTM D4595 procedures suggest that stiffness be calculated by the offset secant procedure. This method is used to eliminate the initial settling-in portion of a unit tension–strain curve. However, it was observed that the preloading technique

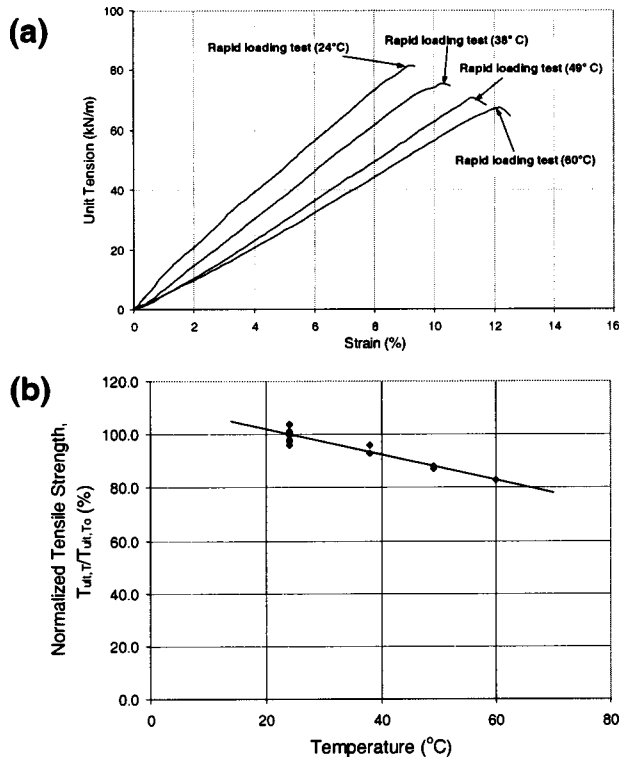

Fig. 3. Effect of temperature: (a) on typical unit tension–strain curves and (b) on ultimate tensile strength

used in this study virtually eliminated settling in for the woven geotextile. Consequently, a linear stress–strain curve was obtained for each test, allowing determination of the stiffness using a linear regression of all data points up to failure. Fig. 3(a) shows a typical unit tension–strain curve obtained at room temperature (24°C). An average stiffness of 9.0 kN/m was obtained from the eight wide-width tests. The standard deviation of stiffness is 0.3 kN/m, yielding a coefficient of variability of 3.7%. The average strain at failure was 9.4%.

Characterization of Rapid Loading at Elevated Temperatures

In addition to tensile tests at room temperature, wide-width tensile tests were performed at the exposure temperatures used during accelerated (SIM) creep and multistage tests. The tensile tests at elevated temperature allowed quantification of the sensitivity of tensile strength to temperature. Wide-width tensile tests at elevated temperatures also provided reference strength values for quantification of loss of tensile strength after a sustained period of creep. Specifically, the residual tensile strength and stiffness measured at elevated temperatures after sustained creep should be compared to the $T_{ult,T}$ and stiffness determined by wide-width tensile tests at the same temperature. Prior to tensile loading, specimens were subjected to elevated temperatures in the environmental chamber in order to achieve thermal equilibrium. Thermal equalization commenced upon completion of preloading (before rapid loading). The preload was maintained constant throughout the thermal equalization period.

Two wide-width tensile tests were performed at each elevated temperature used for the SIM exposures (38, 49, and 60 °C). The average $T_{ult,T}$ values obtained at 38, 49, and 60 °C were 75.9, 70.8, and 67.1 kN/m, respectively (Table 1). Fig. 3(a) shows typical unit tension–strain curves obtained at these temperatures. As observed in the figure, an increase in temperature leads to an apparent decrease in tensile strength, decrease in stiffness, and increase in strain at rupture. These results are in agreement with the trends reported by Bush (1990). Fig. 3(b) summarizes the relationship between tensile strength and temperature for the woven PP geotextile tested in this study. The results show a linear response characterized by a decrease of 0.6% of T_{ult,T_0} per °C of increasing temperature.

Table 1. Reference Tensile Strength Values

Temperature (°C)	$T_{ult,T0}$ (kN/m)
24	80.5
38	75.9
49	70.8
60	67.1

Characterization of Creep Strain

Accelerated (SIM) creep tests were performed at 20 and 30% of the T_{ult,T_0} to characterize the creep strain response. The SIM tests conducted in this study employed 2-h dwell times at each of four exposure temperatures (24, 38, 49, and 60°C). A rapid ramp-up loading with a constant strain rate of approximately 10%/min was initially applied until reaching the target creep load, T_{CR}. The second stage of the test involved maintaining the constant load to characterize the creep behavior. The SIM approach was used for this portion of the test. Fig. 4(a) shows the creep curves obtained from five identical accelerated creep tests for load levels corre-

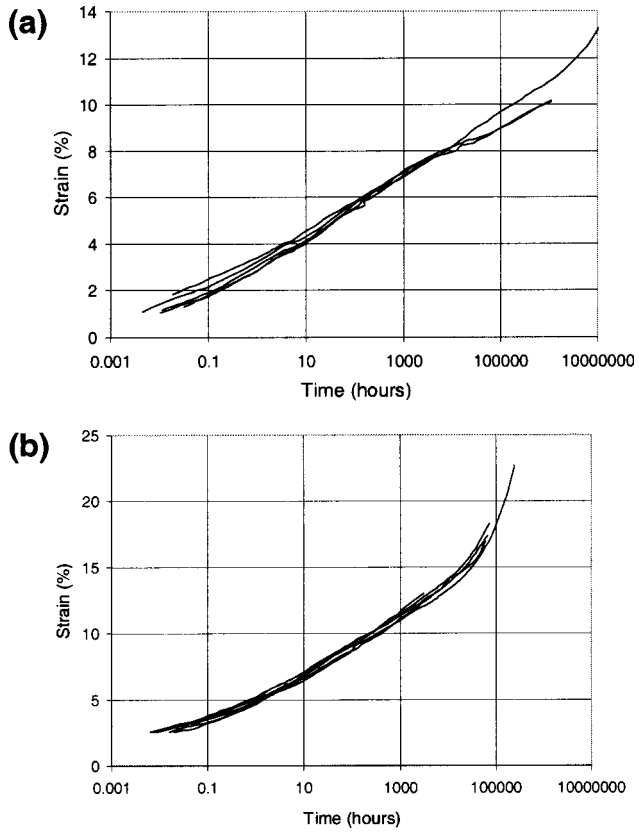

Fig. 4. Stepped isotherm method creep–strain curves obtained for: (a) a load equal to 20% of $T_{ult,T0}$ and (b) a load equal to 30% of $T_{ult,T0}$

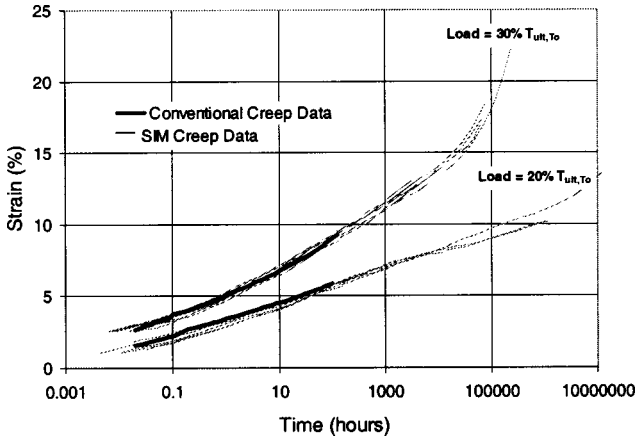

Fig. 5. Comparison between stepped isotherm method and conventional creep data

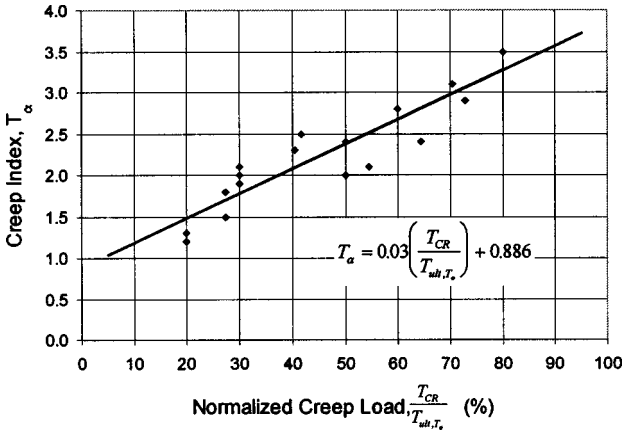

Fig. 6. Creep index as a function of creep load

sponding to 20% of $T_{ult,T0}$. In addition, Fig. 4(b) shows the creep curves obtained from seven identical accelerated creep tests for load levels corresponding to 30% of $T_{ult,T0}$. The creep results are remarkably consistent indicating very good repeatability at different creep load levels.

By conducting an 8-h long SIM test, creep strains corresponding to periods of sustained loading ranging from 10 to 100 years could be obtained. The data confirm accepted creep patterns, including an increasing creep strain rate for increasing load levels. Characterization of the geosynthetic strain is of interest for deformation analyses. For a general creep test, the total strain, ε, can be defined as:

$$\varepsilon = \varepsilon_i + \varepsilon_{CR} \tag{5}$$

where ε_i=initial strain due to ramp-up loading; and ε_{CR}=creep strain.

The creep strain, ε_{CR}, can be defined by characterizing the slope of the linear portion of the creep curve, which is defined herein as the creep index, T_α. That is:

$$\varepsilon_{CR} = T_\alpha \log_{10}\left(\frac{t}{t_0}\right) \tag{6}$$

where ε_{CR}=expressed in (%); T_α=creep index; t=arbitrary time; and t_0=time at the end of ramp-up loading.

The creep index, represented by the slope of the creep curves, is dependent upon the load level and equals approximately 1.2% per log time cycle for a creep load of 20% of $T_{ult,T0}$, while the creep index equals approximately 2.0% per log time cycle for a creep load of 30% of $T_{ult,T0}$. T_α is a dimensionless parameter analogous to the secondary compression index, C_α, determined from consolidation testing of soils and used to quantify secondary compression (creep) strains of soils.

In order to validate the accelerated creep tests, data from SIM creep tests was compared against conventional creep data. A 98-h creep test at 20% of $T_{ult,T0}$ and a 123-h creep test at 30% $T_{ult,T0}$ were conducted at room temperature (24°C) to verify the accelerated creep methodology used in this study. The conventional creep tests were conducted at room temperature using the same equipment and procedures as the SIM creep tests. Fig. 5 shows the conventional creep tests along with SIM creep tests conducted using the same creep loads (20 and 30% of $T_{ult,T0}$). The figure shows excellent agreement between the conventional and SIM creep total strains as a function of time.

While creep tests (conventional or accelerated) have been reported to show good repeatability to characterize creep strains (ε_{CR}) as a function of time, the initial strain component, ε_i, has been reported to depend highly on test equipment and loading procedures (Thornton et al. 1999; Baras et al. 2002). The results in Fig. 5 show that use of testing procedures consistent with wide-width tests leads to a remarkably consistent ε_i. To avoid the effects of ε_i on results, the creep index, T_α, rather than the total strain at a given time (e.g., design life) appears to be a more appropriate parameter to quantify the creep response of geosynthetics for design purposes.

Creep index values were also obtained for creep loads over 30% of $T_{ult,T0}$ in this investigation. The relationship between T_α and creep load for the woven PP geotextile evaluated in this investigation is shown in Fig. 6. A linear trend can be fitted to the data, leading to the following relationship:

$$T_\alpha = a + b\left(\frac{T_{CR}}{T_{ult,T0}}\right) \tag{7}$$

where $(T_{CR}/T_{ult,T0})$=normalized creep load expressed in (%); and a and b=constants used to fit the linear trend. For the woven PP geotextile evaluated in this investigation, a=0.886 and b=0.03.

Characterization of Creep Failure

Creep testing programs have been conventionally carried out to define the creep–rupture curve, which defines the time to geosynthetic rupture under a constant sustained load. As previously discussed, creep reduction factors have been typically based upon creep–rupture data. However, creep failure of the geosynthetic reinforcement is defined in this investigation by the point in the strain log time curve where the creep curve deviates from linear behavior on a semilogarithmic plot (Fig. 7). It should be emphasized that creep failure is different than creep rupture (i.e., creep failure does not imply rupture of the geosynthetic specimen). This creep–failure criterion was found to be more objective than a criterion involving identifying the time and strain leading to specimen rupture.

The creep–failure curve of the woven PP geotexile was defined in this study by conducting 14 tests using creep loads ranging from 20 to 80% of $T_{ult,T0}$. Table 2 summarizes results obtained from the testing program implemented to define the creep–failure curve. Strain at failure obtained for a wide range of creep loads falls within a very narrow range, with an average strain of approximately 15.0%. This provides additional evidence that the

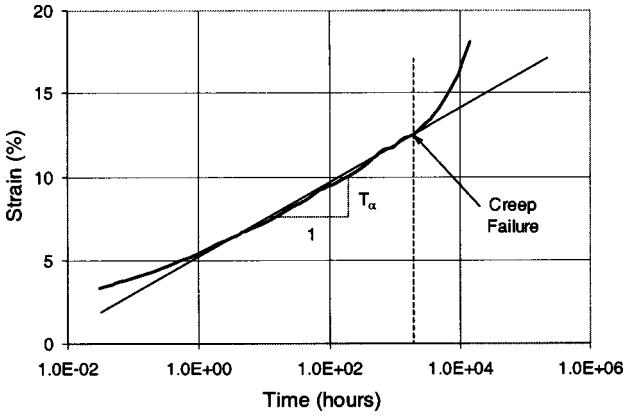

Fig. 7. Definition of creep failure

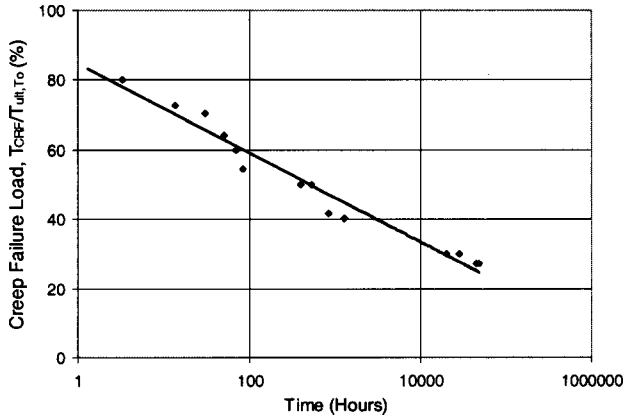

Fig. 8. Creep–failure curve

creep–failure definition used in this study is more consistent than a failure criterion based on specimen rupture. Fig. 8 presents the creep–failure curve obtained for the woven PP geotextile, which shows a well-defined linear trend in a semilogarithmic plot (R^2 = 0.97). The creep-failure curve for this material can be represented by:

$$\frac{T_{CR,F}}{T_{ult,T0}} = 0.85 - 0.056 \log_{10} t \tag{8}$$

where $T_{CR,F}$= creep load leading to creep failure at a given time t.

Characterization of Residual Tensile Strength

The residual strength of geosynthetics can be defined as the tensile strength obtained from rapid loading to rupture conducted after a sustained period of creep. Past studies have reported that geosynthetics retain most of their original tensile strength when loaded to rupture after sustained creep loading. Bernardi and Paulson (1997) presented residual strength data from conventional creep test programs conducted using virgin geogrids as well as high density polyethylene (HDPE) geogrids exhumed from a retaining wall. Orsat et al. (1998) performed rapid loading tests after conventional creep on PET tendons. Zornberg and Kavazanjian (2001) evaluated the residual tensile strength of PP geogrids. Finally, Greenwood et al. (2001) utilized the SIM to define the creep–rupture curve and residual tensile strength of PET geosynthetics. While previous studies have provided significant insight into the residual strength of geosynthetics, they have typically been conducted using comparatively small creep periods (i.e., for strains well below those corresponding to creep failure) or using procedures that are not consistent with wide-width testing.

Multistage tests for determination of residual tensile strength were conducted in this study at the elevated temperatures employed during SIM testing (60°C in most cases). As previously discussed, the tensile strength of geosynthetics shows an apparent decrease with increasing temperature [Fig. 3(b)]. Consequently, the residual tensile strength obtained by rapid loading after sustained creep at elevated temperatures should be compared to the tensile strength obtained from wide-width tests conducted at the same elevated temperatures. This allows quantifying the potential changes in tensile strength due solely to sustained creep loading. Hence, residual tensile strength is reported in this study as a percentage of the tensile strength obtained from wide-width tensile tests conducted at the corresponding elevated temperature.

Rapid loading until specimen rupture was conducted at a constant strain rate (approximately 10%/min) following the desired period of SIM creep loading. Fig. 9 illustrates typical loading paths for multistage tests conducted to define the residual tensile strength after a sustained period of creep loading equal to 30% of

Table 2. Summary of Creep–Failure Test Results

Test ID	Normalized creep load, $T_{CR}/T_{ult,T0}$(%)	Creep index T_α	Time to failure (h)	Strain at failure (%)
CF1	80.1	3.5	3.3	15.0
CF2	72.8	2.9	13.5	15.2
CF3	70.4	3.1	30	16.9
CF4	64.3	2.4	50	14.8
CF5	60.0	2.8	69	16.0
CF6	54.6	2.1	84	14.0
CF7	50.0	2.0	529	15.6
CF8	50.0	2.4	388	16.0
CF9	41.7	2.5	825	14.8
CF10	40.4	2.3	1,274	15.0
CF11	30.0	2.0	19,949	13.5
CF12	30.0	2.1	28,109	15.0
CF13	27.3	1.5	47,904	14.0
CF14	27.3	1.8	44,344	14.6

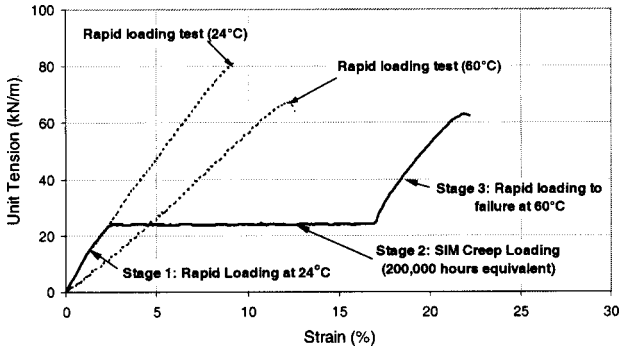

Fig. 9. Comparison between multistage test ($T_{CR}=20\%T_{ult,T0}$) and rapid loading tests with no creep history

$T_{ult,T0}$. The rapid initial loading (Stage 1) was conducted at a temperature of 24°C, the creep loading (Stage 2) was conducted using the SIM over a period of 8 h, and the final rapid loading to rupture (Stage 3) was conducted at a temperature of 60°C. Based upon principles of time–temperature superposition, the data gathered during the 8-hour creep–loading portion of the test corresponds to 200,000 hours of creep loading at a constant temperature of 24°C. The results from wide-width tensile tests conducted at 24°C ($T_{ult,T0}=90.5$ kN/m) and at 60°C ($T_{ult,T0}=67.1$ kN/m) are also shown in the figure. The stiffness obtained for the wide-width tensile test conducted at 24°C agrees with that obtained during initial loading in the multistage test. The stiffness obtained for the wide-width tensile test conducted at 60°C agrees approximately with that obtained during the rapid loading to rupture in the multistage test (although a stiffer response is observed during the initial portion of the rapid loading to rupture in the multistage test). The residual tensile strength in the multistage test ($T_{ult,res}$) of 63.6 kN/m is approximately 95% of the ultimate tensile strength value obtained at 60°C ($T_{ult,T}$).

Consequently, no significant tensile strength loss (i.e., no degradation) took place even after significant creep strain. Fig. 10 compares the response of multistage tests conducted using sustained creep loads of 20 and 30% of $T_{ult,T0}$. Similar residual tensile strength values were obtained in both tests.

Five multistage tests were performed to define the residual tensile strength following sustained creep loading of 20% of $T_{ult,T0}$ (16.1 kN/m.) and seven multistage tests were performed following creep loading of 30% of $T_{ult,T0}$ (24.1 kN/m). Rapid

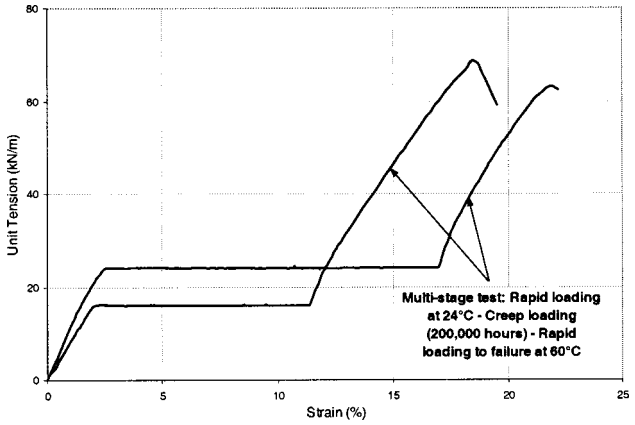

Fig. 10. Multistage tests conducted for determination of residual tensile strength. Creep stages were conducted at 20 and 30% of $T_{ult,T0}$

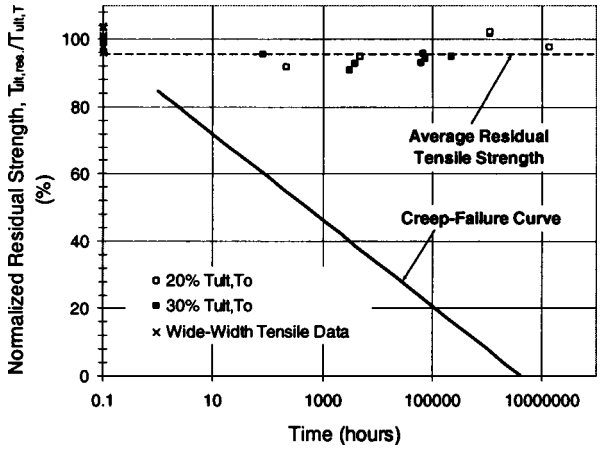

Fig. 11. Residual tensile strength obtained after sustained creep under loads of 20 and 30% of $T_{ult,T0}$

loading to rupture was conducted after various creep time periods. Fig. 11 shows residual tensile strength results obtained from the multistage tests conducted in this study. $T_{ult,res}$ is reported as a percentage of the ultimate tensile strength at the corresponding elevated temperature ($T_{ult,T}$). The results show that the average residual tensile strength is approximately 95% of $T_{ult,T}$ ($T_{ult,res}$ exceeds 90% of $T_{ult,T}$ for every test). The residual tensile strength is observed to be independent of the magnitude and duration of the creep loading. The creep–failure curve is also shown as a reference in Fig. 11. For a given time (e.g., design life), the residual tensile strength results are significantly higher than the tensile values defined by the creep–failure load. Table 3 summarizes the results from the residual tensile strength testing program. The objective of the testing program was to characterize the residual tensile strength for a wide range of strain levels. Consequently, some of the rapid loading tests to characterize $T_{ult,res}$ were conducted after periods of sustained creep beyond those corresponding to creep failure. Initial loading stiffness values reported in Table 3 were obtained under room–temperature conditions, while rapid loading stiffness curves following sustained creep were obtained under elevated temperatures. The stiffness obtained from rapid loading curves after sustained creep at elevated temperature is slightly higher than that obtained from rapid loading curves with no creep loading history at the same elevated temperature.

Design Implications

Current design procedures for GRS structures rely on the use of creep reduction factors defined using creep–rupture curves (Elias et al. 2001). However, lumping different creep aspects (e.g., loss of tensile strength due to creep, creep failure, excessive creep deformations) into a single reduction factor has led to conservative approaches. Accordingly, design of GRS structures should incorporate: (1) A creep reduction factor that accounts for the actual loss in tensile strength, (2) an appropriate factor of safety that accounts for creep failure during the design life of the structure, and (3) a deformation analysis that accounts for potentially excessive long-term deformations. It should be noted that the creep tests performed for this research were performed in isolation. It is recognized, though, that unconfined creep testing may overestimate the long-term creep deformations that would occur under soil confinement (e.g., McGown et al. 1982; Wu and Hel-

Table 3. Summary of Residual Tensile Strength Results

Test ID	Normalized creep load, $T_{CR}/T_{ult,T0}$(%)	Time of creep loading (h)	Creep index T_α	Normalized residual tensile strength (%)	Stiffness (kN/m)	
					Initial	After creep
RS1	20	213	1.2	91.8	8.5	9.1
RS2	20	4,709	1.3	94.8	8.9	8.2
RS3	20	1,096,121	1.2	101.5	5.1	7.1
RS4	20	1,096,914	1.2	102.4	7.5	7.2
RS5	20	13,848,396	1.3	97.6	7.1	5.5
RS6	30	82	1.9	95.5	7.6	10.9
RS7	30	3,058	1.9	90.9	7.7	9.7
RS8	30	3,721	2.0	92.5	8.4	10.9
RS9	30	61,631	2.1	93	8.2	7.7
RS10	30	66,587	2.1	95.8	7.5	8.0
RS11	30	72,603	2.0	94.1	8.7	8.0
RS12	30	245,984	2.1	94.7	8.6	7.8
			Average:	95.4	7.8	8.3

wany 1996). Thus, design approaches based on unconfined tests are conservative, as they do not account for the potentially beneficial effect of soil confinement.

Accounting for Tensile Strength Loss in Design

The long-term design reinforcement tension load, $T_{allowable}$, has been defined as (Elias et al. 2001):

$$T_{allowable} = \frac{T_{ult}}{RF_{CR} \cdot RF_D \cdot RF_{ID} \cdot FS} \quad (9)$$

where RF_{CR}=creep reduction factor; RF_D=durability reduction factor, RF_{ID} is the installation damage reduction factor; and FS= overall factor of safety accounting for uncertainties (e.g., in the tensile strength properties). The FS does not account for creep–failure considerations.

The creep reduction factor, RF_{CR}, has been defined as the ratio between the creep–rupture load for a given design life, t_{dl}, and the ultimate tensile strength of the reinforcement. The creep–failure curve shown in Fig. 8 suggests that the material investigated in this study would exhibit early creep failure under relatively low load levels. In this case, for a design life of 30 years (2.6×10^5 h), the allowable creep load is only 15% of the $T_{ult,T0}$. Accordingly, the creep reduction factor would be 6.7 if current procedures are followed (Elias et al. 2001). This implies that rapid events, such as seismic loading, would lead to failure if the tensile forces induced by such rapid event exceed 15% of $T_{ult,T0}$. This contradicts data presented in Fig. 11, where $T_{ult,res}$ is only slightly below $T_{ult,T0}$ for creep loads extending for time periods as long as 100 years. The comparatively high $T_{ult,res}$ values reported herein for PP geotextiles is consistent with results reported for PP geogrids (Zornberg and Kavazanjian 2001) and for PET geosynthetics (Orsat et al. 1998; Greenwood et al. 2001). Consequently, current creep reduction factors (defined from creep–rupture curves rather than from quantification of the residual tensile strength) are very conservative, particularly if used for rapid (e.g., earthquake) loading conditions.

The average residual tensile strength for the geotextile used in this study is 95% of $T_{ult,T0}$. Hence, a creep reduction factor $RF_{Cr}=1.0/0.95=1.05$ should be used for this material. This value is significantly below 6.7, which is the value defined using the creep–failure curve, and also well below the default value of 5.0 recommended for PP materials (Elias et al. 2001).

Accounting for Creep Failure in Design

Design should also verify that the long-term design reinforcement tension load, $T_{allowable}$, does not lead to creep failure within the design life of the structure, t_{dl}. The factor of safety with respect to creep failure, $FS_{CR,F}$ can be defined as:

$$FS_{CR,F} = \frac{T_{CR,F}(t_{dl})}{T_{allowable}} \quad (10)$$

where $T_{CR,F}(t_{dl})$=creep–failure load for the design life, t_{dl}, which can be estimated using relationships such as the one indicated by Eq. (8). Considering that the creep–failure curve obtained using unconfined specimens is a conservative estimate of the creep response of the geosynthetic under the confinement of soil, a $FS_{CR,F}=1$ is deemed adequate. Thus, $T_{allowable}$ should be adopted based on requirements established not only to prevent tensile breakage [Eq. (9)], but also to prevent creep failure [Eq. (10)].

Accounting for Creep Deformations in Design

Design criteria in current practice often establish a maximum total geosynthetic strain that should not be exceeded during a structure lifetime. Deformability analyses could be performed to quantify expected long-term deformations in a GRS structure. However, design criteria establishing a maximum allowable creep strain rate seems more appropriate. Specifically, the creep index, T_α, can be used to quantify the expected creep strains in a practical manner suitable for design purposes. Accordingly, design criteria could involve defining the maximum allowable creep index of the reinforcement products considered for design. The maximum allowable creep index criterion for a project can be established, for a given design life, from the maximum creep strain values acceptable for the structure. The use of a maximum allowable creep index criterion is simple, and an improvement over the current state of the practice, which typically does not account for creep deformability in design (even though very high RF_{CR} values are used to penalize the geosynthetic ultimate tensile strength).

The creep index, T_α, increases with increasing creep load. Consequently, creep tests should be conducted at different load levels to characterize the rate of creep strain as a function of creep load for a given geosynthetic product. The creep index can be adequately characterized using the same set of creep tests conducted as part of testing programs conducted to determine the

creep-failure curve of a product. The relationship between T_α and T_{CR} is defined by Eq. (7) and presented in Fig. 6 for the woven PP geotextile used in this study. Characterization of the linear trend defining T_α for a given geosynthetic may help to minimize the need for extensive creep testing.

In summary, a three-phase approach is suggested to account for creep in the design of GRS structures. This includes: (1) Quantification of a RF_{CR} to account for the loss in tensile strength (using tests conducted to quantify the residual tensile strength), (2) quantification of $FS_{CR,F}$ to account for creep–failure mechanisms (using tests conducted to quantify creep failure), and (3) quantification of T_α to account for expected creep deformations (using conventional or accelerated creep tests). This approach is expected to lead to more realistic, less conservative designs than the current approach of using a creep reduction factor obtained from creep–rupture curves. Accelerated tests using time–temperature superposition techniques can be used to characterize the creep-induced loss in tensile strength, creep failure, and creep deformation in a time frame suitable for practical applications.

Summary and Conclusions

A tensile testing program including wide-width tensile tests (conducted at both room and elevated temperatures), conventional and accelerated creep tests (conducted using time–temperature superposition techniques), and multistage tests (involving initial rapid loading, subsequent creep loading, and final rapid loading to rupture) was conducted using a woven PP geotextile. The test equipment included a high-capacity load frame, roller grips capable of accommodating 200-mm wide specimens, and a temperature-controlled environmental chamber. The main findings drawn from this investigation include:

- The use of wide-width specimens, roller grips, and preloading procedures led to very good repeatability of results from accelerated multistage tensile tests. This included good repeatability of initial strains (prior to creep loading), which have been reported to show significant scatter.
- The SIM conducted using 200-mm wide specimens and roller grips was successful to characterize PP geosynthetics in spite of their high creep susceptibility. The SIM results obtained in this study compared well with those obtained from conventional (room temperature) creep tests.
- A creep–failure curve was defined by identifying the point where the creep curve deviates from linear behavior in a semilogarithmic scale. The strain at failure was observed to fall within a very narrow range (approximately 15% for the geosynthetic investigated in this study) for a wide range of creep loads (20 to 80% of $T_{ult,T0}$).
- The creep index, T_α, describing creep strain as a function of time, was found to respond linearly with creep loads. Use of T_α instead of the total strain at a given design life is deemed adequate for use as design criterion to account for creep deformations.
- The ultimate tensile strength at elevated temperature, $T_{ult,T}$, was found to respond linearly with temperature. Characterization of $T_{ult,T}$ at elevated temperatures allows proper quantification of tensile strength losses after sustained creep accelerated using the SIM.
- A consistent evaluation of creep-induced loss in tensile strength and changes in stiffness can be obtained using comparatively short tests conducted at elevated temperatures. The residual tensile strength and stiffness obtained at elevated temperatures should be compared to reference values from wide-width tensile tests conducted at identical temperatures.
- The residual tensile strength of the woven PP geotextile investigated in this study exceeded 90% of $T_{ult,T}$ after long-term creep loading at 20 and 30% of $T_{ult,T0}$. The residual tensile strength was found to be independent of the creep load and of the creep time period.
- A three-phase approach involving quantification of the geosynthetic residual strength (to define RF_{CR}), creep–failure response (to define $FS_{CR,F}$), and creep strain rates (to define T_α) is proposed. This should lead to a more realistic design than the current approach of using a creep reduction factor determined from creep–rupture curves.

Acknowledgments

The writers are indebted to Rob Swan (SGI Testing Services, LLC) and Dean Sandri (Soil Retention Systems, Inc.) for their invaluable assistance during this study. Support provided by the National Science Foundation under Grant CMS-0401494 is gratefully acknowledged.

Notation

The following symbols are used in this paper:

a_T = shift factor;
C_1, C_2 = empirical constants;
C_α = secondary compression index;
E = activation energy;
FS = factor of safety;
$FS_{CR,F}$ = factor of safety against creep failure;
k = kinetic rate constant;
k_0 = pre-exponential rate constant;
R = universal gas constant;
RF_{CR} = reduction factor for creep;
RF_D = reduction factor for degradation;
RF_{ID} = reduction factor for installation damage;
T = elevated temperature;
T_0 = reference temperature;
T_α = creep index;
$T_{allowable}$ = long-term allowable reinforcement tension;
T_{CR} = creep load;
$T_{CR,F}$ = creep failure load;
$T_{CR,R}$ = creep rupture load;
t = time;
t_0 = time at the end of ramp-up loading;
t_{dl} = design life;
$T_{ult,res}$ = residual tensile strength;
$T_{ult,T0}$ = ultimate tensile strength at reference temperature, T_0;
$T_{ult,T}$ = ultimate tensile strength at elevated temperature, T;
$\dot{\varepsilon}$ = strain rate;
ε_{CR} = creep strain; and
ε_i = initial strain.

References

Baras, L. C. S., Bueno, B. S., and Costa, C. M. L. (2002). "On the evaluation of stepped isothermal method for characterizing creep

properties of geotextiles." *Proc., 7th Int. Conf. on Geosynthetics*, A. A. Balkema, 1515–1518.
Bernardi, M., and Paulson, J. (1997). "Is creep a degradation phenomenon?" *Mechanically stabilized backfill*, 289–294.
Bush, D. I. (1990). "Variation of long-term design strength of geosynthetics in temperatures up to 40°C." *Proc., 4th Int. Conf. on Geotextiles, Geomembranes, and Related Products*, 673–676.
Elias, V., Christopher, B. R., and Berg, R. R. (2001). "Mechanically stabilized earth walls and reinforced soil slopes design and construction guidelines." *Publication No. FHWA NH-00-043*.
Farrag, K. (1998). "Development of an accelerated creep testing procedure for geosynthetics. II: Analysis." ASTM *Geotech. Test. J.*, 21(1), 38–44.
Ferry, J. D. (1980). *Viscoelastic properties of polymers*, 3rd Ed., Wiley, New York.
Geosyntec Consultants. (1996). "Summary report of findings." Rep. No. *SWP-9*, Prepared for New Cure, Inc., Operating Industries, Inc. Landfill, Monterey Park, Calif.
Geosynthetic Research Institute GRI. (1997). "Grip types for use in the wide width testing of geotextiles and geogrids." Interim Standards, *GT9*, Geosynthetic Research Institute, Folsum, Pa.
Greenwood, J. H., Jones, C. J. F. P., and Tatsuoka, F. (2001). "Residual strength and its application to design of reinforced soil in seismic areas." *Proc. Int. Symp. in Earth Reinforcement, IS-Kyushu*, Balkema, Rotterdam, The Netherlands, 37–42.
Koerner, R. M., Lord, A. E., Jr., and Hsuan, Y. H. (1992). "Arrhenius modeling to predict geosynthetic degradation." *Geotext. Geomembr.*, 11(2), 151–183.
Leshchinsky, D., and Fowler, J. (1990). "Laboratory measurement of load-elongation relationship of high-strength geotextiles." *Geotext. Geomembr.*, 9(2), 145–164.
McGown, A., Andrawes, K. Z., and Kabir, M. H. (1982). "Load-extenstion testing of geotextiles confined in soil." *Proc., 2nd. Int. Conf. Geotextiles*, Vol. 3, 793–798.
Myles, B. and Carswell, I. G. (1986). "Tensile testing of geotextiles." *Proc. of the Third International Conference on Geotextiles*, 713–718.
Orsat, P., Khay, M., and McCreath, M. (1998). "Study on creep rupture of polyester tendons: Full-scale tests." *Proc., 6th Int. Conf. on Geosynthetics*, Atlanta, 675–678.
Thornton, J. S., Allen, S. R., Thomas, R. W., and Sandri, D. (1998a). "The stepped isothermal method for time–temperature superposition and its application to creep data on polyester yarn." *Proc., 6th Int. Conf. on Geosynthetics*, Atlanta, 699–706.
Thornton, J. S., Paulson, J. N., and Sandri, D. (1998b). "Conventional and stepped isothermal methods for characterizing long term creep strength of polyester geogrids." *Proc., 6th Int. Conf. on Geosynthetics*, Atlanta, 691–698.
Thornton, J. S., Sprague, C. J., Klompmaker, J., and Wedding, D. B. (1999). "The relationship of creep curves to rapid loading stress-strain curves for polyester geogrids." *Proc., Geosynthetics '99*, 735–744.
Wu, J. T. H., and Helwany, S. M. B. (1996). "A performance test for assessment of long-term creep behavior of soil-geosynthetic composites." *Geosynthet. Int.* 3(1), 107–124.
Zornberg, J. G., and Kavazanjian, E. (2001). "Prediction of the performance of a geogrid-reinforced slope founded on solid waste," Japanese Geotechnical Society. *Soils Found.*, 41(6), 1–16